


BRIEF REPORT

Importance of tubulin detyrosination in platelet biogenesis

Sylvie Moog¹ | Léa Mallo¹ | Anita Eckly¹ | Carsten Janke^{2,3} | Aurora Pujol^{4,5,6} |
 Pablo Iruzubieta^{7,8,9} | Adolfo López de Munain^{7,8} | Marie-Jo Moutin¹⁰ |
 Catherine Strassel¹ | François Lanza¹ | Quentin Kimmerlin¹¹ 

¹Université de Strasbourg, Institut National de la Santé et de la Recherche Médicale (INSERM), Etablissement Français du Sang (EFS) Grand-Est, Biologie et Pharmacologie des Plaquettes Sanguines (BPPS), Unité Mixte de Recherche (UMR)-S1255, Fédération de Médecine Translationnelle de Strasbourg (FMTS), Strasbourg, France

²Université Paris-Saclay, Centre National de la Recherche Scientifique (CNRS), Unité Mixte de Recherche (UMR) 3348, Orsay, France

³Institut Curie, Université Paris Sciences & Lettres, Centre National de la Recherche Scientifique (CNRS), Unité Mixte de Recherche (UMR) 3348, Orsay, France

⁴Neurometabolic Diseases Laboratory, Bellvitge Biomedical Research Institute (IDIBELL), Barcelona, Spain

⁵Centre for Biomedical Research on Rare Diseases (CIBERER), Instituto de Salud Carlos III, Madrid, Spain

⁶Catalan Institution of Research and Advanced Studies (ICREA), Barcelona, Spain

⁷Department of Neurology, Donostia University Hospital, Biodonostia Health Research Institute, Donostia-San Sebastián, Spain

⁸CIBERNED Centro de Investigación Biomédica en Red en Enfermedades Neurodegenerativas-Instituto de Salud Carlos III (CIBER-CIBERNED-ISCIII), Madrid, Spain

⁹Department of Neurology and Neurosurgery, Montreal Neurological Hospital and Institute, McGill University, Montreal, Quebec, Canada

¹⁰Université Grenoble Alpes, Institut National de la Santé et de la Recherche Médicale (INSERM) U1216, Centre National de la Recherche Scientifique (CNRS), Grenoble Institut Neurosciences, Grenoble, France

¹¹Department of Biomedicine, Experimental Hematology, University Hospital Basel and University of Basel, Basel, Switzerland

Correspondence

Quentin Kimmerlin, Department of Biomedicine, Experimental Hematology, University Hospital Basel and University of Basel, Basel 4031, Switzerland.
 Email: quentin.kimmerlin@unibas.ch

Funding information

This work was supported by the University of Strasbourg and the University of Basel

Abstract

Background: The functional diversity of microtubules is regulated through the expression of distinct α - and β -tubulin isoforms together with several posttranslational modifications, a concept known as tubulin code. Tubulin detyrosination is a reversible posttranslational modification that consists of the removal of the genetically encoded C-terminal tyrosine residue of most α -tubulins. While this modification has been observed in the megakaryocyte lineage, its importance remains poorly understood in platelet biogenesis.

Objectives: To assess the role of α -tubulin detyrosination in platelet biogenesis.

Methods: The responsible enzymes and the relative abundance of detyrosinated α -tubulins were monitored by quantitative reverse transcription-polymerase chain reaction and Western blotting, respectively, in human cultured megakaryocytes and platelets differentiated from CD34⁺ hematopoietic stem and progenitor cells. The function of α -tubulin detyrosination was assessed in human cultured megakaryocytes treated with the VASH-SVBP inhibitor EpoY, and in mice constitutively inactivated for *Svbp* (which encodes the cofactor of the VASH detyrosinases).

Manuscript handled by: Kellie Machlus

Final decision: Kellie Machlus, 27 February 2025

© 2025 The Author(s). Published by Elsevier Inc. on behalf of International Society on Thrombosis and Haemostasis. This is an open access article under the CC BY license (<http://creativecommons.org/licenses/by/4.0/>).

Results: Transcriptional analysis identified VASH1-SVBP and MATCAP as the predominant detyrosinases in the megakaryocyte lineage. During megakaryocyte maturation, their transcript levels progressively increased and correlated with the accumulation of detyrosinated α -tubulins. Remarkably, inhibition of VASH1-SVBP by EpoY abolished tubulin detyrosination, establishing VASH1-SVBP as the main functional detyrosinase in megakaryocytes. More importantly, EpoY enhanced proplatelet formation and platelet production *in vitro*. These *in vitro* data were confirmed *in vivo* in SVBP-deficient mice, which exhibited an increase in platelet counts.

Conclusion: These findings reveal, for the first time, a role for tubulin detyrosination in proplatelet formation, thereby expanding our understanding of the megakaryocyte tubulin code beyond tubulin isoforms.

KEYWORDS

megakaryocytes, microtubules, posttranslational modifications, tubulin carboxypeptidase, tyrosine

1 | INTRODUCTION

Blood platelets are small nonnucleated cellular fragments that are essential to arrest bleeding. They are produced in the bone marrow by large polyploid cells known as megakaryocytes, which arise from hematopoietic stem cells through megakaryopoiesis [1]. This intricate process is characterized by several cycles of endomitosis, the expansion of an intracellular membrane network, and the formation of specialized granules. It culminates in the formation of long cytoplasmic protrusions termed proplatelets, which fragment within the vasculature to generate platelets. The precise mechanisms regulating these events remain elusive.

Microtubules are hollow cylindrical polymers that are composed of α - and β -tubulin heterodimers. They are involved in a wide range of cellular functions such as cell division, intracellular trafficking, and cell motility [2]. In the megakaryocyte lineage, microtubules are particularly important in the final stages of platelet biogenesis. They promote the elongation of proplatelets *in vitro* by sliding against one another to push against the membrane of megakaryocytes [3]. They also provide essential structural support to circulating platelets by assembling a unique submembraneous ring-like structure, called marginal band. This distinctive array maintains the typical flat, disc-shaped morphology of platelets, thereby guarantying their hemostatic properties [4].

The functional diversity of microtubules is regulated through the expression of distinct α - and β -tubulin isoforms together with several posttranslational modifications, a concept known as tubulin code [5]. Among tubulin isoforms, α 4A-, α 8-, and β 1-tubulin play important roles in megakaryocytes and platelets. Disruption of any of these isoforms lead to abnormal megakaryocyte maturation, proplatelet formation, and platelet morphology in mice and humans [6]. In contrast, the importance of tubulin posttranslational modifications is poorly understood. Tubulin acetylation appears to be dispensable for the megakaryocyte lineage [7], while polymodifications of β 1-tubulin have

been proposed to influence the localization of motor proteins in megakaryocytes [8]. Little is known, however, about the role of other tubulin modifications.

Tubulin detyrosination is a reversible posttranslational modification that consists of the removal of the genetically encoded C-terminal tyrosine residue of α -tubulins [9]. This process is carried out by several enzymes termed detyrosinases, with VASH1 and VASH2 in complex with their obligate cofactor SVBP [10,11], and the more recently identified MATCAP (TMCP1) and TMCP2 [12,13]. The reverse reaction is catalyzed by the TTL enzyme [14]. Interestingly, megakaryocytes and platelets have been shown to contain detyrosinated microtubules [15,16]. However, whether they ensure specific functions remains to be established. In this study, using both pharmacologic and genetic models, we provide evidence for a role of tubulin detyrosination in the regulation of proplatelet formation. This finding sheds light on the significance of tubulin posttranslational modifications in platelet biogenesis and underscores the importance of the tubulin code in the megakaryocyte lineage.

2 | MATERIAL AND METHODS

2.1 | Mice

SVBP-deficient mice were previously described [17]. All protocols followed the guidelines of the Committee on the Ethics of Animal Experiments of the University of Strasbourg.

2.2 | Isolation and differentiation of human CD34⁺ cells

Human CD34⁺ cells were recovered from leukodepletion filters (Etablissement Français du Sang (EFS)-Grand Est) and differentiated

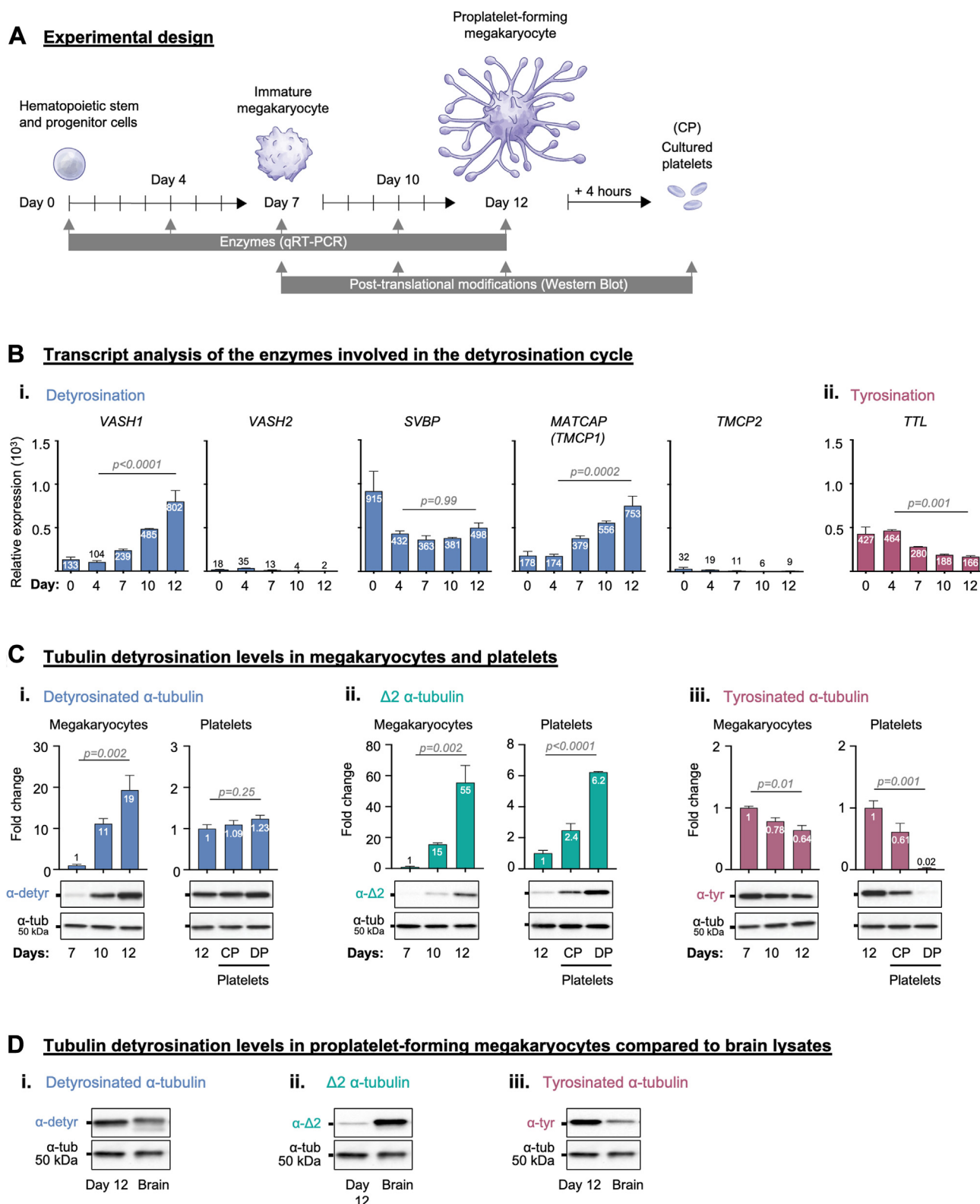


FIGURE 1 Kinetics of tubulin deetyrosination during human platelet biogenesis *in vitro*. (A) Experimental design. (B) quantitative reverse transcription PCR analysis of every known enzyme involved in tubulin deetyrosination/tyrosination (VASH1, VASH2, SVBP, MATCAP, TMCP2, and TTL) during platelet biogenesis. Relative gene expression was determined at different stages of megakaryocyte differentiation *in vitro*, from hematopoietic progenitors (day 0), differentiating megakaryocyte progenitors (day 4), immature megakaryocytes (day 7), and mature megakaryocytes (day 10) to proplatelet-forming megakaryocytes (day 12). Values were normalized to TBP (TATA Binding Protein) using the $\Delta\Delta Ct$ method. Bar graphs representing the mean \pm standard error of the mean. $n = 3$. Statistical analysis was conducted using a 1-way analysis of variance followed by Tukey's honestly significant difference *post hoc* test. (C) Western blot analysis of (i) detyrosinated, (ii) $\Delta 2$, and (iii)

into megakaryocytes and platelets as described [18]. EpoY (SML2301, Merck) was added (20 μ M) at the indicated time points.

2.3 | Isolation and differentiation of mouse Lin-hematopoietic stem and progenitor cells

Bone marrow cells were obtained from the femurs, tibias, and iliac crests. Lineage depletion was performed with the EasySep Mouse Hematopoietic Cell Isolation Kit (Stem Cell Technologies). Lin⁻ cells were cultured as described [19].

2.4 | Bone marrow explant

Marrows were flushed out of mouse femurs, cut into transverse sections, and incubated in culture chambers containing Tyrode's buffer, 5% mouse serum, and 1% penicillin-streptomycin-glutamine [20]. Megakaryocytes were observed after 6 hours.

2.5 | Blood platelet isolation

Washed platelets were prepared from acid citrate dextrose-anticoagulated blood as previously established [21].

2.6 | Light-transmission aggregation and flow cytometry platelet activation

Light-transmission aggregometry and flow cytometry were performed as previously described [4].

2.7 | qRT-PCR

RNA was extracted using the RNeasy Mini kit (Qiagen). Reverse transcription was performed using the RT² Easy First Strand Kit (Qiagen). Quantitative reverse transcription-polymerase chain reactions (qRT-PCRs) were performed in triplicate against *VASH1* (5'-TCGGTGCTGGACGTGGAGC-3' and 5'-CCGTCCCTTGCCAATCTTGA-3'), *VASH2* (5'-GCAGCTGGTCCTCAACGTCTCA-3' and 5'-CACTTG-CAGGTTTCAGGATCTTCATT-3'), *SVBP* (5'-GCAGGAGCTGAAGCAGAGACAA-3' and 5'-GCTGCTGCTCCAGTTCTGTCAT-3'), *MATCAP* (5'-ACCATCGA TTTCCCGTTGCT-3' and 5'-CCCGGGTATTATCCAG

CACC-3'), and *TMCP2* (5'-CGACTCTGACTATCAATGTGTCC-3' and 5'-GGCTGCTGGAGGTTGTTAAT-3') as described elsewhere [22]. Values were normalized to *TBP* ($\Delta\Delta$ ct method).

2.8 | Western blotting

Samples were lysed in Laemmli buffer containing 10 mM dithiothreitol, boiled, separated by sodium dodecyl sulfate-polyacrylamide gel electrophoresis, and transferred onto nitrocellulose membranes. Membranes were incubated with primary anti- α -tubulin (1:5000, clone DM1A, T6199, Merck), antidyrosinated α -tubulin (1:3000, Merck, Ab3201), anti- Δ 2- α -tubulin (1:3000, Merck, Ab3203), or antityrosinated α -tubulin (1:1500, clone TUB-1A2, T9028, Merck), followed by HRP-coupled secondary antibodies for 2 hours, and then incubated with Clarity enhanced chemiluminescence+ (Bio-Rad Laboratories) for 3 minutes and visualized with Chemidoc MP (Bio-Rad Laboratories). Quantification was performed by densitometry using the Bio-Rad ImageLab Software (Bio-Rad Laboratories).

2.9 | Immunofluorescence

Samples were fixed in 4% paraformaldehyde, cytospun, permeabilized, and incubated with antidyrosinated α -tubulin (1:400, Merck, Ab3201), followed by 4 μ g/mL of Alexa647-coupled anti-immunoglobulin G secondary antibody in combination with Alexa488-coupled anti- α -tubulin antibody (1:150, clone DM1A, 53-4502-82, ThermoFischer Scientific) and 2 μ g/mL of Alexa547-coupled anti-CD42c antibody (clone RAM1, EFS-Grand Est). Samples were mounted and examined under a confocal Leica SP8 inverted microscope and a 63 \times oil objective. Images were analyzed with ImageJ software (National Institutes of Health).

2.10 | Mouse blood count

EDTA anticoagulated blood was analyzed with the SCIL Vet ABC Plus Hematology Analyzer (SCIL Animal Care Company).

2.11 | Transmission electron microscopy

Samples were prepared as described [4] and examined at 120 kV under a JEOL 2100Plus Transmission Electron Microscope (FEI).

tyrosinated α -tubulins during platelet biogenesis. Relative levels of modified α -tubulins were determined at different stages of megakaryocyte differentiation *in vitro* and compared between immature megakaryocytes (day 7), mature megakaryocytes (day 10), and proplatelet-forming megakaryocytes (day 12); or proplatelet-forming megakaryocytes (day 12), cultured platelets (CP), and human donor-derived washed platelets (DP). The signal intensity of the modified α -tubulins was estimated by densitometry and normalized to that of total α -tubulin. Results are expressed as fold change. Bar graphs represent the mean \pm SEM. $n = 3$. Statistical analysis was conducted using a one-way analysis of variance, followed by Tukey's honestly significant difference *post hoc* test. (D) Representative Western blot of (i) detyrosinated, (ii) Δ 2, and (iii) tyrosinated α -tubulins in proplatelet-forming megakaryocytes (day 12) and brain lysates, with total α -tubulin used as loading control. $n = 3$.

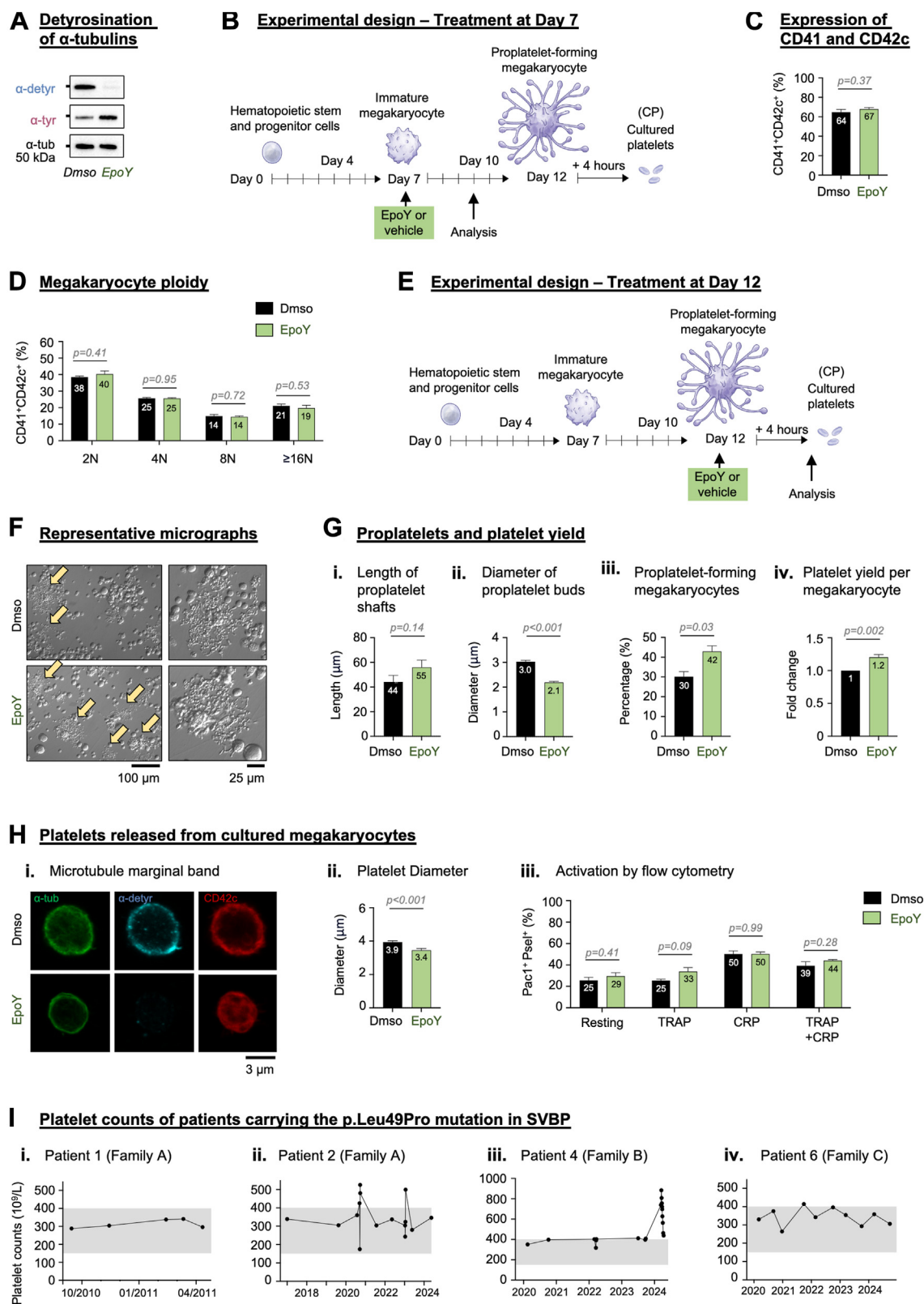


FIGURE 2 Platelet biogenesis in EpoY-treated human cultured megakaryocytes. (A) Western blot analysis of detyrosinated and tyrosinated α -tubulins in proplatelet-forming megakaryocytes treated with dimethyl sulfoxide (DMSO) (0.1 %) or EpoY (20 μ M) for 4 hours. (B) Experimental design for the treatment of immature megakaryocytes (at day 7) with DMSO (0.1 %) or EpoY (20 μ M) for 3 days. (C) Flow cytometry analysis of the CD41⁺ CD42c⁺ megakaryocytes after the treatment of immature megakaryocytes (at day 7) for 3 days with DMSO (0.1 %) or EpoY (20 μ M). Results are expressed as percentage. Bar graphs representing the mean \pm SEM. $n = 3$. Statistical analysis was conducted using a Student's t -test. (D) Flow cytometry analysis of the ploidy levels (2N, 4N, 8N, or ≥ 16 N) of CD41⁺ CD42c⁺ megakaryocytes

2.12 | Bone marrow analysis by flow cytometry

Bone marrow cells were stained as described [23], recorded with a 5-laser Aurora (Cytek), and analyzed using FlowJo 10 (Treestar).

2.13 | Ethics statement

Human studies followed the Declaration of Helsinki. Blood samples and leukodepletion filters were obtained from volunteer donors who provided written informed consent to the EFS-Grand Est.

2.14 | Statistical analysis

Statistical comparisons were performed as indicated in the figure legends.

3 | RESULTS AND DISCUSSION

3.1 | Kinetics of tubulin detyrosination during platelet biogenesis

To account for the presence of detyrosinated microtubules in the megakaryocyte lineage, one possible contributing factor is the substantial proportion of α 4A-tubulin, an isotype synthesized without the typical C-terminal tyrosine [24]. The enzymatic machinery may additionally favor tubulin detyrosination as megakaryocytes mature, a possibility that has not yet been evaluated. To address this question, we characterized the kinetics of tubulin detyrosination in human CD34⁺-derived cultured megakaryocytes and platelets. First, we followed by qRT-PCR the transcripts of all known enzymes involved in this modification at several defined stages of megakaryocyte differentiation, which correspond to CD34⁺ hematopoietic stem and progenitor cells (day 0), differentiating megakaryocyte progenitors (day 4), immature

megakaryocytes (day 7), mature megakaryocytes (day 10), and proplatelet-forming megakaryocytes (day 12; Figure 1A). Then, we correlated the enzyme transcript levels to those of detyrosinated α -tubulins by Western blot in maturing megakaryocytes (days 7-12), cultured platelets and washed platelets from healthy donors (DP).

Transcriptional analysis revealed that the expression of the detyrosinases VASH1 and MATCAP (TMCP1) increased during megakaryocyte maturation, whereas the expression of VASH2 and TMCP2 was barely detectable, and that of the cofactor SVBP remained stable (Figure 1Bi). Interestingly, this coincided with a concomitant decrease in the expression of TTL, which encodes the enzyme that restores the C-terminal tyrosine residue of α -tubulins (Figure 1Bii). This profile of expression therefore suggests that α -tubulins become progressively more detyrosinated as megakaryocytes differentiate, a process likely mediated by VASH1-SVBP and/or MATCAP. Direct observation of the modification by Western blot corroborates this hypothesis and revealed a progressive accumulation of both detyrosinated α -tubulins and Δ 2- α -tubulins (which are generated by removing the exposed C-terminal glutamate of detyrosinated tubulins; Figure 1Ci, ii). This was accompanied by a marked reduction in tyrosinated tubulins (Figure 1Ciii). Taken together, it can thus be postulated that the combined accumulation of the C-terminal tyrosine-lacking α 4A-tubulin and increased detyrosination by VASH1-SVBP and/or MATCAP generates microtubules that progressively reach a highly detyrosinated state during platelet biogenesis. Analysis of mouse brain lysates, where detyrosination is abundant [9,25], reinforces this claim by showing that detyrosinated α -tubulins are at least as prevalent in megakaryocytes as they are in the brain (Figure 1D).

3.2 | Importance of tubulin detyrosination in human platelet biogenesis

To identify the enzyme(s) responsible for the detyrosination of α -tubulins, we next treated human megakaryocytes with the selective

after treatment of immature megakaryocytes (at day 7) for 3 days with DMSO (0.1 %) or EpoY (20 μ M). Results are expressed as percentage. Bar graphs representing the mean \pm SEM. $n = 3$. Statistical analysis was conducted using a Student's t -test. (E) Experimental design for the treatment of proplatelet-forming megakaryocytes (at day 12) with DMSO (0.1%) or EpoY (20 μ M) for 4 hours. (F) Representative DIC micrographs of proplatelet-forming megakaryocytes (at day 12) treated with DMSO (0.1%) or EpoY (20 μ M) for 4 hours. The left panels correspond to a large field of view, with arrows indicating proplatelet-forming megakaryocytes. The right panels correspond to a close-up view of a proplatelet-forming megakaryocyte. Scale bar = 100 μ m (left panel) and 25 μ m (right panel). (G) Analysis of proplatelet-forming megakaryocytes (at day 12) treated with DMSO (0.1%) or EpoY (20 μ M) for 4 hours. (i) Length of proplatelet shafts. Results are expressed in μ m. Bar graphs representing the mean \pm SEM. $n = 4$. Statistical analysis was conducted using a Student's t -test. (ii) Diameter of proplatelet buds. Results are expressed in micrometers. Bar graphs representing the mean \pm SEM. $n = 4$. Statistical analysis was conducted using a Student's t -test. (iii) Percentage of proplatelet-forming megakaryocytes. Results are expressed as fold change. Bar graphs representing the mean \pm SEM. $n = 4$. Statistical analysis was conducted using a paired Student's t -test. (iv) Platelet yield per megakaryocyte assessed by flow cytometry. Results are expressed as fold change. Bar graphs representing the mean \pm SEM. $n = 4$. Statistical analysis was conducted using a Student's t -test. (H) Analysis of platelets released from proplatelet-forming megakaryocytes (at day 12) treated with DMSO (0.1 %) or EpoY (20 μ M) for 4 hours. (i) Representative confocal micrograph of a cultured platelet. Microtubules were stained for total α -tubulin (green, left) and detyrosinated α -tubulin (cyan, middle). Platelet surface was stained for CD42c (red, right). Scale bar = 3 μ m. (ii) Diameter of cultured platelets. Results are expressed in μ m. Bar graphs representing the mean \pm SEM. $N = 4$. Statistical analysis was conducted using a Student's t -test. (iii) Flow cytometry analysis of P-selectin⁺ Pac1⁺ platelets activated with 100 μ M of thrombin receptor activator peptide-6, 10 μ g/mL of synthetic cross-linked collagen-related peptide, or both. (I) Platelet counts of 4 patients from 3 independent families carrying the p.Leu49Pro mutation in SVBP, previously reported in ref. 27. Results are expressed in 10^9 /L over time. (i, ii) Patients 1 and 2 from family A. (iii) Patient 4 from family B. (iv) Patient 6 from family C.

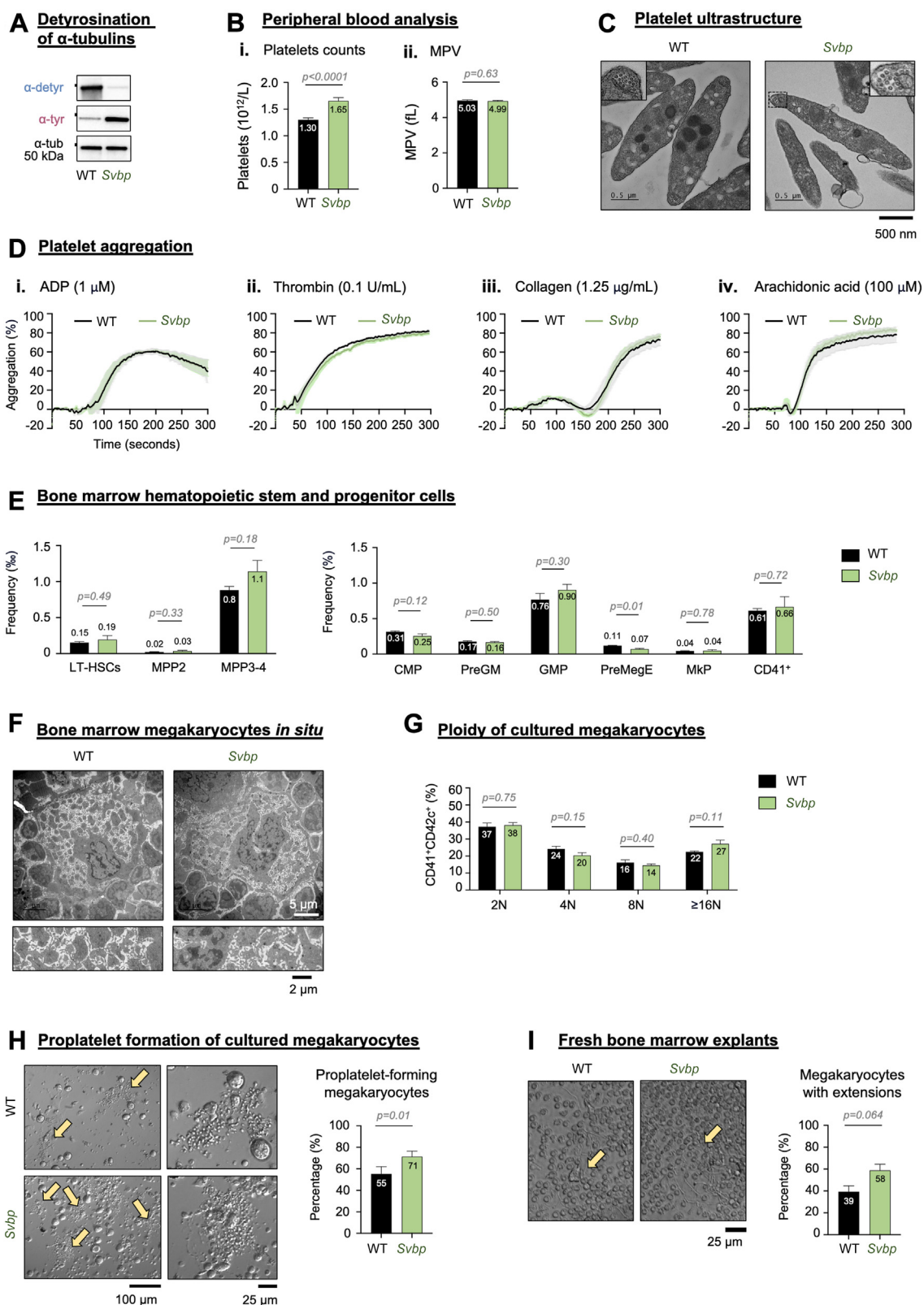


FIGURE 3 Platelet biogenesis in SVBP-deficient mice. (A) Western blot analysis of detyrosinated and tyrosinated α -tubulins in WT and SVBP-deficient washed platelets. (B) Peripheral blood analysis of WT and SVBP-deficient mice. (i) Platelet counts. Results are expressed in $10^{12}/L$. Bar graph representing the mean \pm SEM. $n > 20$ per strain. Statistical analysis was conducted using a Welch's t-test. (ii) Mean platelet volumes (MPV). Results are expressed in fL. Bar graph representing the mean \pm SEM. $n > 20$ per strain. Statistical analysis was conducted using a Student's t-test. (C) Representative transmission electron micrographs of WT and SVBP-deficient platelets. The upper right corner shows a cross-sectioned microtubule marginal band. Scale bar = 500nm. (D) Light-transmission aggregation profiles of WT or SVBP-deficient washed

VASH-SVBP inhibitor EpoY [26]. Remarkably, EpoY completely abolished tubulin detyrosination (Figure 2A). This observation therefore indicates that VASH1-SVBP is likely the main functional detyrosinase in the megakaryocyte lineage. Despite this inhibitory effect, treatment of immature megakaryocytes with EpoY (from day 7 to day 10, Figure 2B) had no measurable impact on their maturation (Figure 2C, D). However, treatment of mature megakaryocytes that had already started to extend proplatelets (at day 12 for 4 hours, Figure 2E) further enhanced proplatelet formation (Figure 2F, G). While a trend toward longer proplatelet shafts with smaller buds was observed (Figure 2Gi, ii), EpoY significantly increased the percentage of proplatelet-forming megakaryocytes from 30% to 42% (Figure 2Giii) and their platelet yield (Figure 2Giv). Platelets released from treated megakaryocytes exhibited no visible abnormalities, with the exception of a slightly smaller size, and successfully assembled a marginal band and activated in response to different agonists (Figure 2H). Taken together, our findings demonstrate that detyrosination of α -tubulins is orchestrated mainly by VASH1-SVBP in megakaryocytes and that this modification can dynamically fine-tune the process of proplatelet formation *in vitro*. In support of this conclusion, we analyzed platelet counts from 4 patients across 3 independent families carrying the p.Leu49Pro mutation in SVBP. Despite only leading to a partial decrease in tubulin detyrosination levels [27], these patients consistently show platelet counts near or slightly above the upper limit of the normal range (Figure 2I).

3.3 | Tubulin detyrosination in platelet biogenesis in mice

To validate our observations, we next analyzed mice constitutively inactivated for *Svbp*, which encodes the chaperone and cofactor of the detyrosinases VASH1/2 [28]. In this model, the absence of SVBP makes both VASH enzymes nonfunctional. As a result, detyrosination of α -tubulins was nearly undetectable in washed platelets of

SVBP-deficient mice, similar to human cultured megakaryocytes treated with EpoY (Figure 3A). This observation thus reinforces the hypothesis that VASH1-SVBP is likely to be the predominant detyrosinase in the megakaryocyte lineage. Interestingly, SVBP-deficient mice displayed a significant increase in platelet counts when compared with their wild-type (WT) littermates (+27%, Figure 3B). No differences were observed in the ultrastructure (Figure 3C) or functions (Figure 3D) of SVBP-deficient platelets. All other examined hematologic parameters were unchanged (Table 1), suggesting that *Svbp* inactivation only affected the megakaryocyte lineage in the hematopoietic system.

To explain the increased platelet counts of SVBP-deficient mice, we next evaluated whether megakaryopoiesis was affected. Flow cytometry and transmission electron microscopy analysis of the bone marrow however revealed no significant abnormalities in megakaryocyte differentiation and maturation (Figure 3E, F). Next, we assessed the ability of cultured megakaryocytes to extend proplatelets. Remarkably, although SVBP-deficient megakaryocytes exhibited normal ploidy (Figure 3G), the percentage of proplatelet-forming megakaryocytes was significantly higher when compared with WT controls (increased from 55% to 71%, Figure 3H). A similar trend was observed in megakaryocytes that matured within their native environment using an *ex vivo* bone marrow explant model (Figure 3I). Taken together, these results are consistent with our findings on EpoY-treated human megakaryocytes and could account for the elevated platelet counts of SVBP-deficient mice. In summary, our results show that, while VASH1-SVBP and detyrosinated α -tubulins are not essential for megakaryocyte differentiation and maturation, they can fine-tune proplatelet formation *in vitro* and influence platelet counts *in vivo*. The underlying mechanism remains, however, unclear but could involve dynein regulation to promote microtubule sliding, a process that is essential for proplatelet elongation *in vitro* [3,29]. In conclusion, our study sheds new light on a previously unrecognized role of α -tubulin detyrosination in the formation of proplatelets *in vitro*, underscoring the importance of the tubulin code in the

platelets ($3 \times 10^5/\mu\text{L}$) in response to either 1 μM of ADP, 0.1 U/mL of thrombin, 1.25 $\mu\text{g/mL}$ of type I Horm collagen, or 100 μM arachidonic acid. Results are expressed as the percentage of light-transmission over time (in seconds). Graphs representing the mean \pm SEM. $n = 3$. (E) Flow cytometry analysis of hematopoietic stem and progenitor cell populations in freshly isolated bone marrow cell suspensions (red blood cell-lysed). Results are expressed in frequency. Bar graphs representing the mean \pm SEM. $n = 3$. Statistical analysis was conducted using a Student's *t*-test. LT-HSCs = Lin⁻C-kit⁺Sca-1⁺CD48⁺CD150⁺Epcr⁺, MPP2 = Lin⁻C-kit⁺Sca-1⁺CD48⁺CD150⁺, MPP3-4 = Lin⁻C-kit⁺Sca-1⁺CD150⁺, CMP = Lin⁻C-kit⁺Sca-1⁺CD16/32⁺CD34⁺, GMP = Lin⁻C-kit⁺Sca-1⁺CD16/32⁺CD34⁺, PreGM = Lin⁻C-kit⁺Sca-1⁺CD41⁺CD16/32⁺CD105⁺CD150⁺, PreMegE = Lin⁻C-kit⁺Sca-1⁺CD41⁺CD16/32⁺CD105⁺CD150⁺, MkP = Lin⁻C-kit⁺Sca-1⁺CD41⁺CD150⁺. (F) Representative transmission electron micrographs of mature stage III megakaryocytes observed in bone marrow sections. Scale bar = 5 μm . (G) Flow cytometry analysis of the ploidy levels (2N, 4N, 8N, or $\geq 16\text{N}$) of CD41⁺ CD42c⁺ megakaryocytes obtained from WT and SVBP-deficient bone marrow Lin⁻ hematopoietic stem and progenitor cells after 3 days of culture. Results are expressed as percentage. Bar graphs representing the mean \pm SEM. $n = 3$. Statistical analysis was conducted using a Student's *t*-test. (H) Analysis of cultured megakaryocytes obtained from WT and SVBP-deficient bone marrow Lin⁻ hematopoietic stem and progenitor cells after 4 days of culture. (Left) Representative DIC micrographs. The left panels correspond to a large field of view, with arrows indicating proplatelet-forming megakaryocytes. The right panels correspond to a close-up view of a proplatelet-forming megakaryocyte. Scale bar = 100 μm (left panel) and 25 μm (right panel). (Right) Percentage of proplatelet-forming megakaryocytes. Results are expressed as percentage. Bar graphs representing the mean \pm SEM. $n = 5$. Statistical analysis was conducted using a paired Student's *t*-test. (I) Analysis of megakaryocytes in the periphery of bone marrow explants after 6 hours in the incubation chamber. (Left) Representative phase-contrast micrograph, with the arrow pointing toward a proplatelet-forming megakaryocyte. Scale bar = 25 μm . (Right) Percentage of megakaryocytes presenting with proplatelet-like extensions. Results are expressed as percentage. Bar graphs representing the mean \pm SEM. $n = 3$. Statistical analysis was conducted using a paired Student's *t*-test. WT, wildtype.

TABLE Peripheral blood parameters of SVBP-deficient mice.

	Platelets ($10 \times 10^9/L$)	Mean platelet volume (fL)	Red blood cells ($10 \times 10^{12}/L$)	White blood cells ($10 \times 10^9/L$)	Hematocrit (%)	Hemoglobin (g/L)
Wildtype mice	1300.65 \pm 35.76	5.03 \pm 0.04	7.542 \pm 0.38	20.63 \pm 1.14	35.00 \pm 1.75	122.59 \pm 5.68
SVBP-deficient mice	1654.29 \pm 62.07	4.99 \pm 0.03	7.89 \pm 0.26	20.38 \pm 0.96	36.31 \pm 1.22	125.00 \pm 4.09
Significance	$P < .0001$	$P = .63$	$P = .36$	$P = .79$	$P = .47$	$P = .69$

megakaryocyte lineage. Finally, our study also highlights EpoY as an attractive compound to enhance the production of human cultured platelets, offering a cost-effective option that could be used to scale up platelet production for transfusion purposes [30].

ACKNOWLEDGMENTS

This work was supported by the University of Strasbourg and the University of Basel. We warmly thank Ketty Knez-Hippert for her valuable advice on animal welfare and management, Jean-Yves Rinckel and Fabienne Proamer for their exceptional technical expertise in electron microscopy, and Ivan Bièche and his team for the qRT-PCR.

AUTHOR CONTRIBUTIONS

S.M. performed experiments and analyzed and discussed the data. L.M. performed experiments and analyzed and discussed the data. A.E. performed experiments and analyzed the data. C.J. analyzed and discussed the data. A.P. collected and provided patient data and analyzed and discussed the data. P.I. collected and provided patient data and analyzed and discussed the data. A.L.d.M. collected and provided patient data and analyzed and discussed the data. M.-J.M. analyzed and discussed the data. C.S. designed the study and analyzed and discussed the data. F.L. designed the study and analyzed and discussed the data. Q.K. designed the study, performed experiments, analyzed and discussed the data, and wrote the manuscript.

DECLARATION OF COMPETING INTERESTS

There are no competing interests to disclose.

ORCID

Quentin Kimmerlin  <https://orcid.org/0000-0002-1999-782X>

REFERENCES

- [1] Boscher J, Guinard I, Eckly A, Lanza F, Léon C. Blood platelet formation at a glance. *J Cell Sci*. 2020;133:jcs244731. <https://doi.org/10.1242/jcs.244731>
- [2] Akhmanova A, Kapitein LC. Mechanisms of microtubule organization in differentiated animal cells. *Nat Rev Mol Cell Biol*. 2022;23:541–58.
- [3] Bender M, Thon JN, Ehrlicher AJ, Wu S, Mazutis L, Deschmann E, Sola-Visner M, Italiano JE, Hartwig JH. Microtubule sliding drives proplatelet elongation and is dependent on cytoplasmic dynein. *Blood*. 2015;125:860–8.
- [4] Kimmerlin Q, Moog S, Yakusheva A, Ziessel C, Eckly A, Freund M, Závodszy G, Knapp Y, Mangin P, Lanza F. Loss of $\alpha 4A$ - and $\beta 1$ -tubulins leads to severe platelet spherocytosis and strongly impairs hemostasis in mice. *Blood*. 2022;140:2290–9.
- [5] Janke C, Magiera MM. The tubulin code and its role in controlling microtubule properties and functions. *Nat Rev Mol Cell Biol*. 2020;21:307–26.
- [6] Kimmerlin Q, Strassel C, Eckly A, Lanza F. The tubulin code in platelet biogenesis. *Semin Cell Dev Biol*. 2023;137:63–73.
- [7] Ribba AS, Batzenschlager M, Rabat C, Buchou T, Moog S, Khochbin S, Bourova-Flin E, Lafanechère L, Lanza F, Sadoul K. Marginal band microtubules are acetylated by α TAT1. *Platelets*. 2021;32:568–72.
- [8] Khan AO, Slater A, MacLachlan A, Nicolson PLR, Pike JA, Reyat JS, Yule J, Stapley R, Rayes J, Thomas SG, Morgan NV. Post-translational polymodification of $\beta 1$ -tubulin regulates motor protein localisation in platelet production and function. *Haematologica*. 2022;107:243–59.
- [9] Sanyal C, Pietsch N, Ramirez Rios S, Peris L, Carrier L, Moutin MJ. The detyrosination/re-tyrosination cycle of tubulin and its role and dysfunction in neurons and cardiomyocytes. *Semin Cell Dev Biol*. 2023;137:46–62.
- [10] Aillaud C, Bosc C, Peris L, Bosson A, Heemeryck P, Van Dijk J, Le Friec J, Boulan B, Vossier F, Sanman LE, Syed S, Amara N, Couté Y, Lafanechère L, Denarier E, Delphin C, Pelletier L, Humbert S, Bogoy M, Andrieux A, et al. Vasohibins/SVBP are tubulin carboxypeptidases (TCPs) that regulate neuron differentiation. *Science*. 2017;358:1448–53.
- [11] Nieuwenhuis J, Adamopoulos A, Bleijerveld OB, Mazouzi A, Stickel E, Celie P, Altelaar M, Knipscheer P, Perrakis A, Blomen VA, Brummelkamp TR. Vasohibins encode tubulin detyrosinating activity. *Science*. 2017;358:1453–6.
- [12] Landskron L, Bak J, Adamopoulos A, Kaplani K, Moraiti M, van den Hengel LG, Song JY, Bleijerveld OB, Nieuwenhuis J, Heidebrecht T, Henneman L, Moutin MJ, Barisic M, Taraviras S, Perrakis A, Brummelkamp TR. Posttranslational modification of microtubules by the MATCAP detyrosinase. *Science*. 2022;376:eabn6020. <https://doi.org/10.1126/science.abn6020>
- [13] Nicot S, Gillard G, Impheng H, Joachimiak E, Urbach S, Mochizuki K, Wloga D, Juge F, Rogowski K. A family of carboxypeptidases catalyzing α - and β -tubulin tail processing and deglutamylation. *Sci Adv*. 2023;9:eadi7838. <https://doi.org/10.1126/sciadv.adi7838>
- [14] Ersfeld K, Wehland J, Plessmann U, Dodemont H, Gerke V, Weber K. Characterization of the tubulin-tyrosine ligase. *J Cell Biol*. 1993;120:725–32.
- [15] Gundersen GG, Bulinski JC. Microtubule arrays in differentiated cells contain elevated levels of a post-translationally modified form of tubulin. *Eur J Cell Biol*. 1986;42:288–94.
- [16] Patel-Hett S, Richardson JL, Schulze H, Drabek K, Isaac NA, Hoffmeister K, Shivasani RA, Bulinski JC, Galjart N, Hartwig JH, Italiano JE Jr. Visualization of microtubule growth in living platelets reveals a dynamic marginal band with multiple microtubules. *Blood*. 2008;111:4605–16.
- [17] Pagnamenta AT, Heemeryck P, Martin HC, Bosc C, Peris L, Uszynski I, Gory-Fauré S, Couly S, Deshpande C, Siddiqui A, Elmonairy AA, Jayawant S, Murthy S, Walker I, Loong L, Bauer P, Vossier F, Denarier E, et al. WGS500 Consortium, Genomics England Research Consortium. Defective tubulin detyrosination causes

- structural brain abnormalities with cognitive deficiency in humans and mice. *Hum Mol Genet.* 2019;28:3391–405.
- [18] Do Sacramento V, Mallo L, Freund M, Eckly A, Hechler B, Mangin P, Lanza F, Gachet C, Strassel C. Functional properties of human platelets derived in vitro from CD34⁺ cells. *Sci Rep.* 2020;10:914.
- [19] Strassel C, Eckly A, Léon C, Moog S, Cazenave JP, Gachet C, Lanza F. Hirudin and heparin enable efficient megakaryocyte differentiation of mouse bone marrow progenitors. *Exp Cell Res.* 2012;318:25–32.
- [20] Guinard I, Lanza F, Gachet C, Léon C, Eckly A. Proplatelet formation dynamics of mouse fresh bone marrow explants. *J Vis Exp.* 2021;171: e62501.
- [21] Cazenave JP, Ohlmann P, Cassel D, Eckly A, Hechler B, Gachet C. Preparation of washed platelet suspensions from human and rodent blood. *Methods Mol Biol.* 2004;272:13–28.
- [22] Bodakuntla S, Schnitzler A, Villablanca C, Gonzalez-Billault C, Bieche I, Janke C, Magiera MM. Tubulin polyglutamylation is a general traffic-control mechanism in hippocampal neurons. *J Cell Sci.* 2020;133:jcs241802. <https://doi.org/10.1242/jcs.241802>
- [23] Usart M, Stetka J, Luque Paz D, Hansen N, Kimmerlin Q, Almeida Fonseca T, Lock M, Kubovcakova L, Karjalainen R, Hao-Shen H, Börsch A, El Taher A, Schulz J, Leroux JC, Dirnhofer S, Skoda RC. Loss of Dnmt3a increases self-renewal and resistance to pegIFN- α in JAK2-V617F-positive myeloproliferative neoplasms. *Blood.* 2024;143:2490–503.
- [24] Strassel C, Magiera MM, Dupuis A, Batzenschlager M, Hovasse A, Pleines I, Guéguen P, Eckly A, Moog S, Mallo L, Kimmerlin Q, Chappaz S, Strub JM, Kathiresan N, de la Salle H, Van Dorsselaer A, Ferec C, Py JY, Gachet C, Schaeffer-Reiss C, et al. An essential role for α 4A-tubulin in platelet biogenesis. *Life Sci Alliance.* 2019;2: e201900309. <https://doi.org/10.26508/lsa.201900309>
- [25] Paturle L, Wehland J, Margolis RL, Job D. Complete separation of tyrosinated, detyrosinated, and nontyrosinatable brain tubulin subpopulations using affinity chromatography. *Biochemistry.* 1989;28: 2698–704.
- [26] Hotta T, Haynes SE, Blasius TL, Gebbie M, Eberhardt EL, Sept D, Cianfrocco M, Verhey KJ, Nesvizhskii AI, Ohi R. Parthenolide destabilizes microtubules by covalently modifying tubulin. *Curr Biol.* 2021;31:900–7.e6.
- [27] Launay N, Espinosa-Alcantud M, Verdura E, Fernández-Eulate G, Ondaro J, Iruzubieta P, Marsal M, Schlüter A, Ruiz M, Fourcade S, Rodriguez-Palmero A, Zulaica M, Sistiaga A, Labayru G, Loza-Alvarez P, Vaquero A, Lopez de Munain A, Pujol A. Altered tubulin detyrosination due to SVBP malfunction induces cytokinesis failure and senescence, underlying a complex hereditary spastic paraplegia. *Aging Cell.* 2025;24:e14355. <https://doi.org/10.1111/accel.14355>
- [28] Wang N, Bosc C, Ryul Choi S, Boulan B, Peris L, Olieric N, Bao H, Krichen F, Chen L, Andrieux A, Olieric V, Moutin MJ, Steinmetz MO, Huang H. Structural basis of tubulin detyrosination by the vasohibin-SVBP enzyme complex. *Nat Struct Mol Biol.* 2019;26:571–82.
- [29] McKenney RJ, Huynh W, Vale RD, Sirajuddin M. Tyrosination of alpha-tubulin controls the initiation of processive dynein-dynactin motility. *EMBO J.* 2016;35:1175–85.
- [30] Ito Y, Nakamura S, Sugimoto N, Shigemori T, Kato Y, Ohno M, Sakuma S, Ito K, Kumon H, Hirose H, Okamoto H, Nogawa M, Iwasaki M, Kihara S, Fujio K, Matsumoto T, Higashi N, Hashimoto K, Sawaguchi A, Harimoto KI, et al. Turbulence activates platelet biogenesis to enable clinical scale ex vivo production. *Cell.* 2018;174: 636–48.e18.